

SUPPORTING INFORMATION

Ultrafast Photo-Induced Ligand Solvolysis of *cis*- [Ru(bipyridine)₂(nicotinamide)₂]²⁺: Experimental and Theoretical Insight into its Photoactivation Mechanism†

Simon E. Greenough^{a§}, Gareth M. Roberts^{a‡§*}, Nichola A. Smith^a, Michael D. Horbury^a, Russell G. Mckinlay^b, Justyna M. Żurek^b, Martin J. Paterson^b, Peter J. Sadler^a and Vasilios G. Stavros^{a*}

^aDepartment of Chemistry, University of Warwick, Library Road, Coventry, CV4 7AL, UK

^bInstitute of Chemical Sciences, Heriot-Watt University, Edinburgh, EH14 4AS, UK

*E-mail: v.stavros@warwick.ac.uk, g.m.roberts@gristol.ac.uk

†Current address: School of Chemistry, University of Bristol, Cantock's Close, Bristol, BS8 1TS, UK

§These authors contributed equally

S1. Electrospray ionisation mass spectrometry (ESI-MS)

Positive-ion mass spectra were obtained on an Agilent 6130 Quadrupole mass spectrometer. An aqueous solution of **1** (40 μM) was irradiated for 50 s with blue light (465 nm). The sample was further diluted with water before injection.

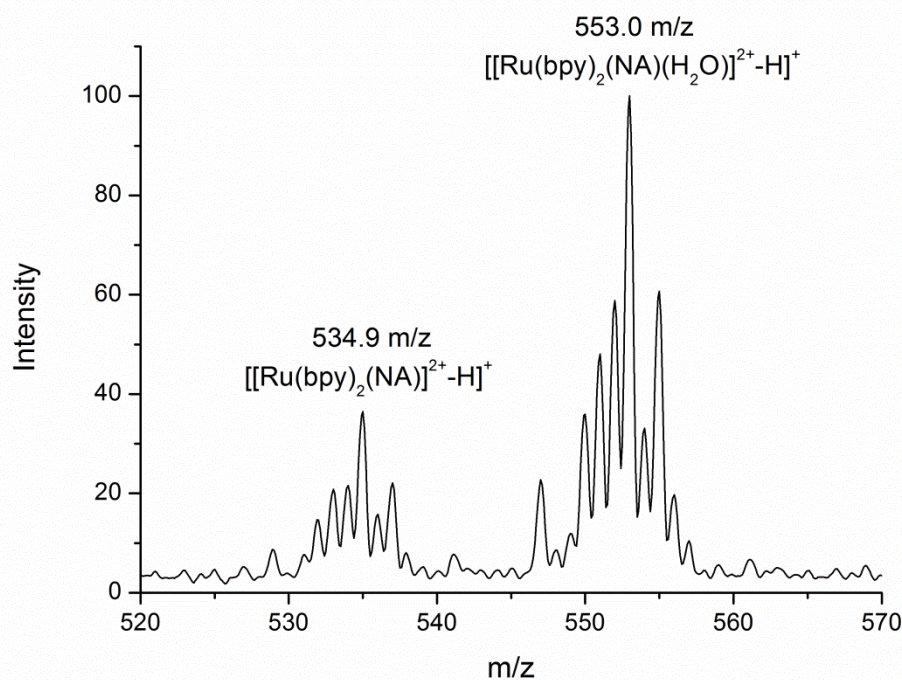


Figure S1. Positive-ion ESI-MS spectrum of **1** in aqueous solution irradiated for 50 s with blue light (465 nm) showing production of $[\text{Ru}(\text{bpy})_2(\text{NA})(\text{H}_2\text{O})]^{2+}$; observed 553.0 m/z, calculated 553.1 m/z for $[\text{Ru}(\text{bpy})_2(\text{NA})(\text{H}_2\text{O})]^{2+}-\text{H}^+$

S2. Calculated molecular orbitals for the *cis*-[Ru(bpy)₂(NA)(H₂O)]²⁺ photoproduct

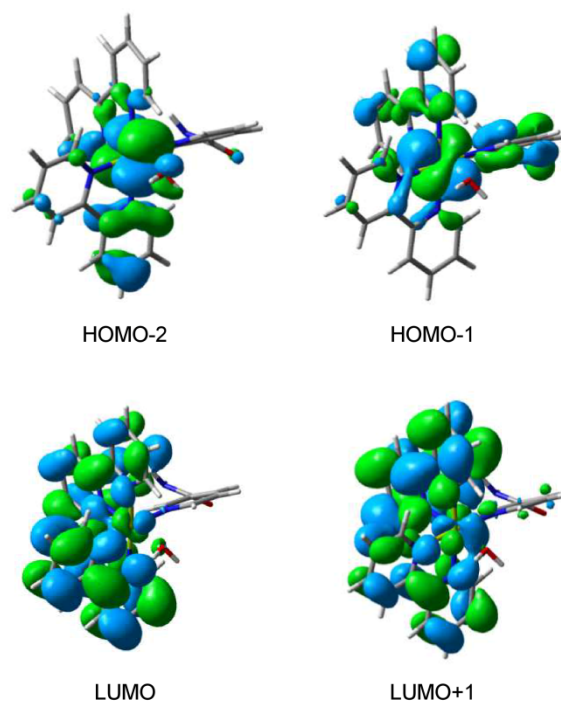


Figure S2. Calculated molecular orbital involved in the (major) orbital transitions associated with the ¹MLCT/³MLCT states of the *cis*-[Ru(bpy)₂(NA)(H₂O)]²⁺ (**2**) photoproduct - see Table 1 of the main text for details. Calculations were performed at the TD-B3LYP/cc-pVTZ-SDD level of theory (see main article for further details).

S3. Ultrafast transient UV/Vis absorption spectra of *cis*-[Ru(bpy)₂(NA)₂]²⁺ in acetone

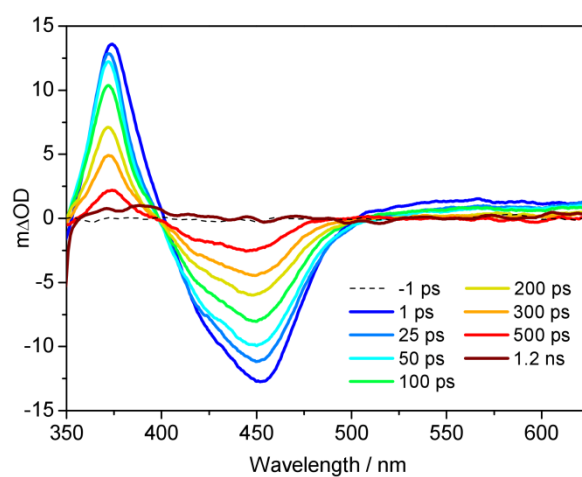


Figure S3. UV/Vis TAS of 890 μM solution of **1** in acetone over pump-probe delay ranges $t = -1$ ps to 1.2 ns, following photoexcitation at 340 nm. The ground state bleach of **1** is spectrally red-shifted in acetone relative to H₂O as evidenced by the static UV/Vis absorption spectra shown in Figure S4 below.

S4. Static UV/Vis absorption spectrum of *cis*-[Ru(bpy)₂(NA)₂]²⁺ in acetone

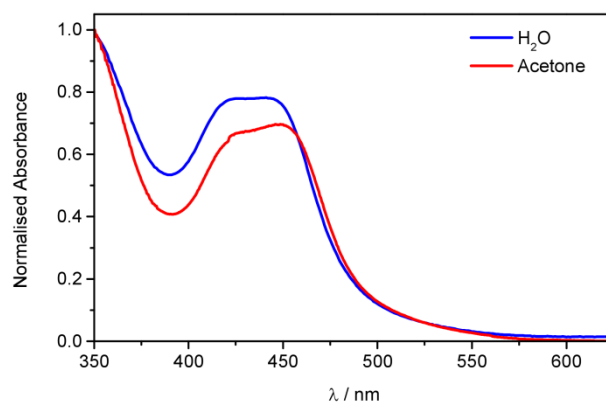


Figure S4. Normalized static UV/Vis absorption spectra of [Ru(bpy)₂(NA)₂]²⁺ (**1**) in both H₂O (blue line) and acetone (red line).

S5. Kinetic analysis of *cis*-[Ru(bpy)₂(NA)₂]²⁺ dissociation in H₂O

Kinetic traces for each of the individual species involved in the photodissociation of **1** (see Figure 6a of main paper) were extracted using a target analysis approach. This was achieved using the recently developed kinetics analysis software package KOALA [1]. For further details on the exact methods used in this fitting program the reader is referred to the comprehensive description of KOALA provided in Ref. 1.

As detailed in the main paper, the final profile of the transient absorption spectra at each time-delay, t , is the result of a convolution of a number individual species involved in the dissociation of **1**. By fitting each individual time-resolved spectrum to basis functions which describe the spectral profile of these species, we can reconstruct the final TAS. To do this, we do not use model functions for the reactant **1** and the mono-aquated photoproduct **2**, but instead directly use the experimentally measured static UV/Vis absorption spectra for these species to accurately account for their spectral profile. For the transient excited ³MLCT state, previous work (see main paper) has reported the excited state absorption profile from this state and we use two Gaussian functions as a basis function to reconstruct reasonably its known absorption profile. Finally, the absorption profile of the PCI species is the dominant unknown in this fitting procedure, which we assume to absorb in the red end of our TAS ($\lambda > 550$ nm) and is modelled with a single Gaussian profile. We acknowledge that the predominant error in our fitting will be born from this assumption, but is guided by complementary theoretical calculations of the PCI absorption profile. The kinetic traces extracted for each of these species are presented in Figure 5 of the main paper. We also briefly note that, in principle a global fitting analysis of our TAS data sets may also have been possible, such as that used by Hauser and co-workers on related ultrafast TAS of [Ru(bpy)₃]²⁺ derivatives [2]. However, such an approach still does not necessarily recover the known absorption profiles of all species involved if simple first order single or bi-exponential kinetics are assumed, particularly when the spectrum is heavily convoluted and the kinetic model is far more complex. This approach would also still require quantum yields to be extracted through simple integration of the bleach recovery, which as we have shown in the main article, will be incorrect as a result of direct overlap between the absorption profiles of **1** and **2**. As a result, analysis of our TAS strongly lends to an *a posteriori* target analysis with KOALA, allowing us to make use of all the known static absorption profiles reported in the main paper.

First (or pseudo-first) order rate equations of the states (shown in Figure 6a) involved in the dynamics of **1** in H₂O:

$$\frac{d[{}^3MLCT_{v>0}]}{dt} = -(k_{VET} + k_d)[{}^3MLCT_{v>0}] \quad [{}^3MLCT_{v>0}](0) = A_0 \quad \text{i}$$

$$\frac{d[{}^3MLCT_{v=0}]}{dt} = k_{VET}[{}^3MLCT_{v>0}] - k_{GSR}[{}^3MLCT_{v=0}] \quad [{}^3MLCT_{v=0}](0) = 0 \quad \text{ii}$$

$$\frac{d[PCI \cdot NA]}{dt} = k_d[{}^3MLCT_{v>0}] - (k_s + k_{GR})[PCI \cdot NA] \quad [PCI \cdot NA](0) = 0 \quad \text{iii}$$

$$\frac{d[PCI]}{dt} = k_s[PCI \cdot NA] - k_{MA}[PCI] \quad [PCI](0) = 0 \quad \text{iv}$$

$$\frac{d[2]}{dt} = k_{MA}[PCI] \quad [2](0) = 0 \quad \text{v}$$

$$\frac{d[1]}{dt} = k_{GSR}[{}^3MLCT_{v=0}] + k_{GR}[PCI \cdot NA] \quad [1](0) = -A_0 \quad \text{vi}$$

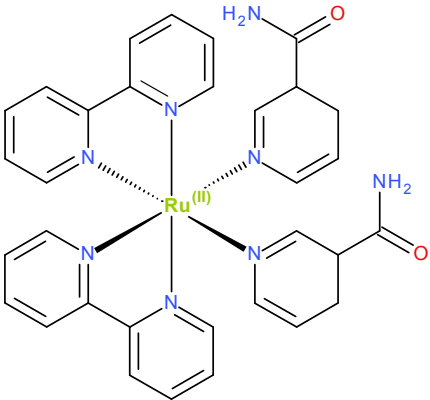
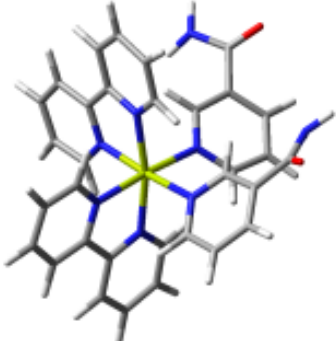
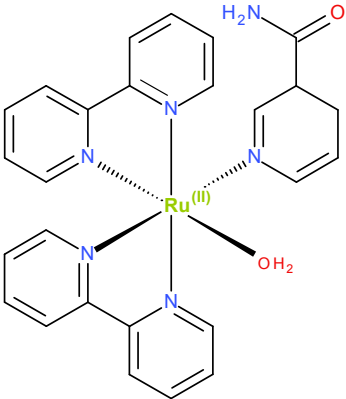
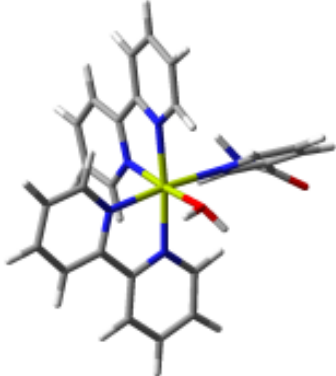
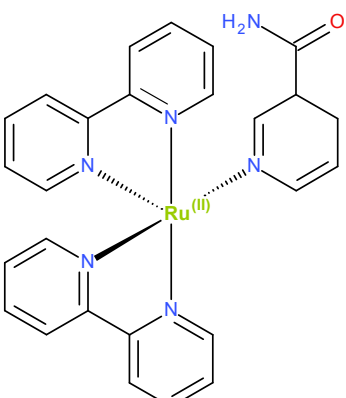
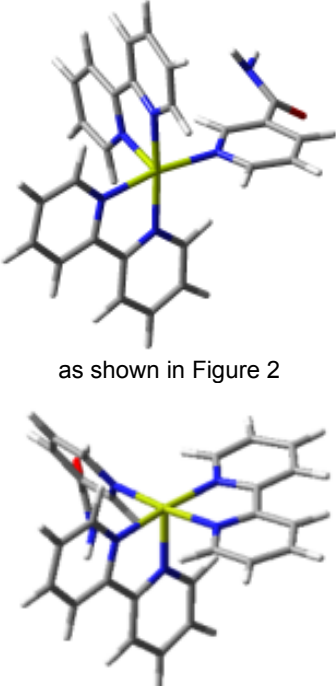
where k_{VET} , k_d , k_s , k_{GSR} , k_{GR} , k_{MA} are rate constants of vibrational energy transfer, dissociation, ligand separation, ground state recovery, geminate recombination and mono-aquation, respectively. As we are blind to ¹MLCT \rightarrow ³MLCT_{v>0} intersystem crossing, and this occurs within our instrumental resolution, we set time $t = 0$ for the kinetic analysis from the event of population of ³MLCT_{v>0}. The initial excited state population transferred from the ¹MLCT following irradiation, $[{}^3MLCT_{v>0}](0)$, is given as A_0 and the ground state bleach of **1** at $t = 0$, $[1](0)$, is thus $-A_0$.

Equations i–vi are solved analytically to give exponential equations that are used to *simultaneously* fit kinetic traces (shown in Figure 5). For example, i gives:

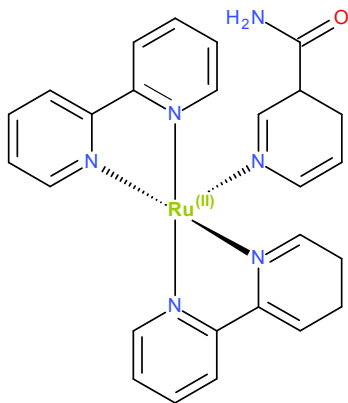
$$[{}^3MLCT_{v>0}](t) = A' e^{-(k_d + k_{VET})t}$$

A' is an amplitude for the exponential function which indicates signal intensity *i.e.* it replaces A_0 (population only) to take into account oscillator strengths of transitions that contribute to the observed signal.

S6. The structures and labelling of the complexes discussed in this paper

Assignment in Main Paper and Chemical Formula	Structural Formula	Ground State Geometry
<p>1 <i>cis</i>-[Ru(bpy)₂(NA)₂]²⁺</p>		
<p>2 <i>cis</i>-[Ru(bpy)₂(NA)(H₂O)]²⁺</p>		
<p>PCI ~or~ pro-<i>cis</i>-PCI [Ru(bpy)₂(NA)]²⁺</p>		<p data-bbox="1091 1576 1321 1601">as shown in Figure 2</p>  <p data-bbox="1091 1935 1321 1960">as shown in Figure 8</p>

pro-*trans*-PCI
 $[\text{Ru}(\text{bpy})_2(\text{NA})]^{2+}$



3
 $\text{cis-}[\text{Ru}(\text{bpy})_2(\text{H}_2\text{O})_2]^{2+}$

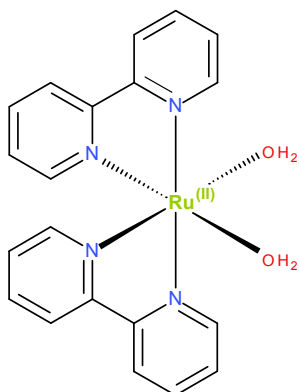


Table S6. The complexes discussed including their assignments in the main paper, chemical formulae, structural formulae and calculated ground state geometric structures. The geometric structures of complexes **1**, **2** and the PCI are included in Figure 2. The structures of the isomers of the PCI, *pro-cis*-PCI and *pro-trans*-PCI, are discussed in Section 3.6 of the main paper with reference to Figure 8. The geometric structure of **3**, which is not involved in the observed dynamics and thus not included in the current analysis, was not calculated.

References

- [1] M.P. Grubb, A.J. Orr-Ewing and M.N.R. Ashfold, *Rev. Sci. Instrum.*, 2014, **85**, 064104.
- [2] Q. Sun, S. Mosquera-Vazquez, L. M. Lawson Daku, L. Guénée, H. A. Goodwin, E. Vauthey and A. Hauser, *J. Am. Chem. Soc.*, 2013, **135**, 13660.